High inorganic content with percolated structure in pore-filling membrane: Platform for functional membranes based on zirconium phosphate

T. Taniuchi,[†] T. Ogawa,[†,*] M. Yoshida, T. Nakazono, and K. N. Ishihara

Department of Socio-Environmental Energy Science, Graduate School of Energy Science, Kyoto University, Yoshida-Honmachi, Sakyo-ku, Kyoto606-8501, Japan.

[*]*Corresponding author. Email: ogawa.takaya.8s@kyoto-u.ac.jp*

Abstract

Organic-inorganic composite membranes are used in various applications, such as proton-conducting electrolyte membranes for PEMFCs. In this study, we filled a polyethylene porous substrate with only but plenty of inorganics (around 48 wt.%), zirconium acetylacetonate, the precursor of zirconium phosphate (ZrP)-based inorganics (AcAc-Zr). It was confirmed that the AcAc-Zr in the substrate was converted into ZrP derivatives in situ, keeping the high contents. TEM-EDS analysis revealed that the pores were continuously filled with ZrP, indicating that ZrP was percolated due to the high contents and the original structure of the porous substrate. The conductivities of these ZrP, ZrHEDP, and ZrATMP films were sufficiently high: on the order of 1 mS cm^{-1} (80°C and 95% relative humidity condition).

Keywords

Zirconium phosphate; Zirconium acetylacetonate; Pore-filling; Organic-inorganic composite membrane; High content

Abbreviations

ZrP, zirconium phosphate; AcAc-Zr, Zirconium acetylacetonate; ZrATMP, zirconium Nitrilotris (methylenephosphonic Acid); ZrHEDP, zirconium 1-Hydroxyethane-1,1-diphosphonic Acid; PEMs, proton exchange membranes; ZrSPP, zirconium sulfophenylphosphonate; SPES, sulfonated poly (arylene ether sulfone)

1. Introduction

Organic-inorganic composite membranes have been attracting attention for decades to improve the performance of membranes in many applications due to the various properties of inorganics. Their applications include membranes used to remove impurities from wastewater [1]–[3], membrane reactors [4]–[6], and separators for batteries such as lithium-ion batteries [7] and redox-flow batteries [8]. Among the several applications, the electrolyte membranes in polymer electrolyte membrane fuel cells (PEMFCs) have attracted significant attention. It is because PEMFCs are promising power generation devices with high energy efficiency and less environmental damage, and are expected to replace internal combustion engines in the future.

However, proton exchange membranes (PEMs) used in PEMFCs have a fatal drawback: proton conductivity severely decreases at low relative humidity (RH) conditions, resulting in reduced energy efficiency. Thus, a lower operating temperature is employed to avoid the excessive evaporation of water. However, lowering the operating temperature leads to CO poisoning of the catalyst [9]. Thus, highly pure fuels are utilized to suppress catalyst poisoning, and water and temperature must be managed to alleviate the decrease in conductivity. These result in extra work and equipment, increasing the cost and decreasing energy efficiency. For this reason, much effort has been devoted to developing membranes to overcome the conductivity dependence on RH [10]–[12]. In particular, it has been demonstrated that inorganic particles in the membrane can adsorb moisture and retain it at high temperatures [13], [14]. Therefore, an organic-inorganic composite membrane is one solution to improve efficiency. Especially zirconium phosphate (ZrP) is promising as a proton-conducting inorganic. ZrP is a layered crystalline, represented as $Zr(HPO_4)_2 \cdot H_2O$, which is

water-insoluble and thermally stable up to about 450℃ [15], [16]. ZrP has a moderate conductivity of 10^{-4}~10^{-3} S cm^{-1} when it is humidified [17], and it can retain hydration water up to about 270℃, depending on crystalline morphology [18].

Although organic-inorganic composite membranes have a variety of possible applications, they have a problem that they become brittle when they contain a large amount of insoluble inorganic particles [19], [20]. It is because too much inorganic induces their agglomerates in a membrane when the composite is formed. As a result, it breaks from the accumulated areas of the inorganic particle when a force is applied to it [21]. However, insoluble inorganic particles are difficult to disperse and avoid agglomeration. So then, a small amount is usually included in a membrane, although high inorganic content is ideal for fully exhibiting the properties of the inorganic. On the other hand, soluble inorganic particles can be well dispersed in organic molecules, suppress the agglomeration, and retain the membrane flexibility. Still, the applications of soluble inorganics are limited since it easily elutes.

Some research produced a membrane containing a large amount of insoluble inorganic particles by making them highly dispersed [22], [23]. However, highly dispersed states do not easily coexist with beneficial morphology, a phase separation structure [24]. In general, PEMs are composed of two phases: the hydrophilic phase for proton conduction and the hydrophobic phase for the stability of the membrane [25]. For example, in membranes with high proton conductivity at high humidity, such as Nafion®, phase separation occurs and forms ion channels, creating continuous proton transfer pathways through the entire membrane [26]. In contrast, the membrane includes fewer pathways under low humidity, decreasing conductivity. Therefore, high content of inorganics with the phase separation structure is vital to keep the sufficient proton transfer pathways.

There is another reason for the decrease in conductivity in a low RH environment. With less H_2O, the conventional proton conduction mechanism, structural diffusion, which inevitably requires water movement, is less likely to occur [27]–[30]. In contrast, the packed-acid mechanism, the mechanism of the proton conduction in a material consisting of a high-density acid structure, does not need water movement and is considered to be less humidity-dependent [27], [28], [31]. Therefore, the packed-acid mechanism improves the conductivity under low RH conditions. Moreover, membranes, where protons conduct via the packed-acid mechanism, are expected to be applied not only to PEMFCs but also to other fields, such as ammonia electrochemical synthesis [32]. The high contents of inorganics are suitable to induce the packed-acid mechanism, expected to overcome the severe dependence of proton conductivity on RH. For these reasons, a method to fabricate a membrane consisting of insoluble inorganics with high content is required.

To overcome the above drawbacks, we focused on a pore-filling method. Pore-filling membrane is prepared by filling a porous substrate with another material. In the case of PEMs fabricated by pore-filling, if the electrolyte is well filled into the pore space, its structure spontaneously becomes phase-separated due to the substrate structure, which has mechanical strength. In other words, a membrane with continuous proton pathways and high durability can be obtained [33]. Furthermore, by reducing the pore size, fuel permeation can be easily reduced, which is one of the advantages [34]. However, it has not been paid much attention as a fabrication method of organic-inorganic composite membranes.

In this study, we proposed a method to fabricate a porous substrate filled with only ZrP derivatives at high contents. Moreover, the membrane morphology is like the phase-separated structure; the phase to retain the membrane form is the substrate with mechanical strength, and the phase for proton conduction is only ZrP without additional electrolyte polymer. Firstly, a zirconium acetylacetonate, the precursor of the ZrP-based inorganics (AcAc-Zr) membrane, was created by filling AcAc-Zr into a porous substrate. Several porous substrates (pore size: 100 nm, 70 nm, 50 nm, 30 nm, 20 nm, and 16 nm) were employed to know the influence of pore size. Intriguingly, the high filling contents were achieved only when the pore size was below 30 nm. Next, we confirmed that the Acac-Zr in the membrane was

converted to ZrP, zirconium amino-tris-methylene-phosphonate (ZrATMP), and zirconium 1-hydroxy ethylidene-1,1-diphosphonate (ZrHEDP), which demonstrated that our methods could fabricate pore-filling membrane with various inorganics. With the membrane filed with a high content of ZrP derivatives, a wide range of applications is expected. For example, as previously mentioned, ZrP has been intensively studied to be included in an electrolyte for PEMFCs [35], [36]. In addition, ZrP derivatives have been intensively studied as an application of catalysts [37], [38], and targeted ion removal [39], [40]. Furthermore, the antimicrobial effect of ZrP derivatives is studied [41], and also ZrP derivatives are considered to be support materials for solid-supported amines (SSAs) [42]. The membrane shape greatly benefits maximizing the properties of ZrP derivatives. Several methods of preparing ZrP membranes have been tried [43], and it turned out to be difficult to make membranes highly filled with ZrP [44], [45]. However, in this study, it was proved that not only ZrP but also ZrATMP/ZrHEDP were highly filled in the substrates in the same method and more, with the phase-separated structure. The proposed method could be a platform for the fabrication of membranes containing various ZrP-based inorganic particles with diverse functions.

2. Experimental

2.1 Materials and chemicals

Commercially available porous polyethylene (PE) substrates (average pore size: 100 nm, 70 nm, 50 nm, 30 nm, 20 nm, 16 nm, thickness 10 μm, porosity 50-55%) were used. 85% Zirconium (IV) Butoxide (Zr-butoxide), 1-Butanol Solution and 2-Propanol were purchased from FUJIFILM Wako Pure Chemical Corp. 99.8% Methanol, Acetylacetone, 1 mol/L-nitric acid, and phosphoric acid were purchased from Nacalai tesque, Inc. 1-hydroxyethane-1,1-diphosphonic acid (ca. 60% in Water, ca. 4.2 mol/L) (HEDPA), nitrilotris (methylenephosphonic Acid) (ca. 50% in Water, ca. 2.2mol/L) (ATMPA) were purchased from Tokyo Chemical Industry Co. LTD.

2.2 Synthesis of AcAc-Zr precursors

According to the previous work [17], AcAc-Zr was synthesized by modifying ZrO_2 with acetylacetone (AcAc). 5.65 g of Zr-butoxide was added to 200 mL of 2-propanol, and stirred for 30 min. 2.50 g of acetylacetone was added to the solution and stirred for three h (molar ratio AcAc/Zr = 2.0). The resulting solution was taken out from the glove bag, 5 mL of 1 molar nitric acid was added, and then stirred for more than 10 hours (molar ratio H^+/Zr = 0.4). The solution was heated to 80 °C using a hot stirrer in a draft chamber to evaporate the solvent, and then, AcAc-Zr powder was obtained.

2.3 Preparation of AcAc-Zr membrane

The AcAc-Zr powder was dissolved in methanol to obtain a 3 wt.% AcAc-Zr methanol solution. The solution was dropped onto a porous substrate and dried at room temperature, and the procedure was repeated about five times until the film became transparent. After the first drop, the substrate was kept in a vacuum at room temperature for about 1 min (vacuum method [46]). The transparent film was washed twice with ultrapure water and dried in a vacuum environment at 80°C for more than 30 min to obtain a transparent AcAc-Zr membrane.

2.4 Fabrication of ZrP/ZrHEDP/ZrATMP membrane

The ZrP, ZrHEDP, and ZrATMP membranes were synthesized by the following procedure. Firstly, phosphonic acid was added to water and methanol to prepare a solution so that i) the amount of phosphorus (P) substance per 1 g of the solution became 5.0×10^{-4} mol/g, and ii) the weight ratio of water to methanol in the solution became 5 : 90. Furthermore, 1 molar nitric acid was added so that the weight ratio of the prepared solution to 1 molar nitric acid became 95 : 5. Sufficient amounts of the phosphonic acid solution were dropped onto the AcAc-Zr membrane and dried at 80°C on a hot stirrer for about 10 minutes. The membrane was turned upside down, the solution was dropped, and then it was dried again. It was washed twice in ultrapure water and dried in a vacuum at 80°C overnight.

2.5 Characterization methods

The pore-filling ratio was calculated from the weight change of the membrane. The calculation formula is shown in equation (1) below, where $W_{after\ filling}$ [g] is the weight of the membrane after pore-filling, and $W_{substrate}$ [g] is the weight of the substrate before pore-filling.

$$\text{Pore} - \text{filling ratio}\ (\%) = \frac{W_{after\ filling} - W_{substrate}}{W_{after\ filling}} \times 100 \quad (1)$$

The transmission wavelengths were measured using FT-IR (Spectrum 100, PerkinElmer, Inc.). In addition, XRD measurements (RINT2100CMJ, Rigaku, Inc.) were performed to identify the crystal structure in the membranes. The acceleration voltage and current were 40 kV and 30 mA, respectively, and the step width and measurement time were 0.050 degrees and 1.0 s/step, respectively. The measurements were performed by the diffractometer method using Cu-Kα radiation (λ = 1.54056 Å).

2.6 SEM/TEM/EDS

The surface of the pore-filling membrane was observed by FE-SEM (SU6600, Hitachi High-Tech Corporation) at an acceleration voltage of 15 kV. A cross-section of the ZrP membrane was obtained by slicing it with a Focused Ion Beam (FIB) device (FB2200, Hitachi High-Tech Corporation), and the structure of inorganic particles in the ZrP membrane was observed using TEM (JEM-2200FS, JEOL Ltd.). Furthermore, the distribution of ZrP in the membrane was investigated by TEM-EDS (JED-2300T, JEOL Ltd.).

2.7 Membrane conductivity measurement

The 80°C and 95%RH were conditioned by an environmental tester (SH-222, Espec Corp.), and the conductivity of the membrane was measured by an AC impedance measurement device (Solartron Analytical 1260A, AMETEK, Inc.). The measurement frequency ranged from 0.1 to 1000 kHz, and the voltage was 100 mV. We employed the 4-probe method. The resistance values were obtained from the Cole-Cole plots (see Appendix), and the conductivity was calculated based on the following equation (3), where the uniform electrode area is A [cm^2], the distance between electrodes is L [cm], the resistance is R [Ω], and the conductivity is σ [Scm^{-1}].

$$\sigma = \frac{1}{R} \times \frac{L}{A} \quad (3)$$

The thickness of the film was measured by a digital micrometer (MDC-25M, Mitutoyo Corporation).

3. Results

3.1 Characterization of the composite membrane

3.1.1 Filling-ratio measurement of ZrP/ZrHEDP/ZrATMP membrane

Fig. 1 shows the steps to fabricate a ZrP pore-filling membrane. The substrate appears white due to the diffuse reflection of light from the numerous pores, but the AcAc-Zr and the ZrP membranes have changed to transparent. It is because the pores are filled with AcAc-Zr or ZrP, and thus the diffuse reflection no longer occurs. The pore-filling ratio of the AcAc-Zr and the ZrP/ZrHEDP/ZrATMP membranes are shown in Fig. 2. Fig. 2(a) indicates substrates with an average pore size of 30 nm can be filled with more than 48wt.% of each compound. On the other hand, Fig. 2(b) shows that the AcAc-Zr membrane with pore sizes of 30 nm or less is highly filled with about 48 wt.% AcAc-Zr. However, after the conversion to ZrP, the 30 nm substrate is the most filled with AcAc-Zr. However, the substrates with pore sizes of 100 nm, 70 nm, and 50 nm failed to be filled, resulting in no transparency change, unlike the change shown in the pictures in Fig. 1.

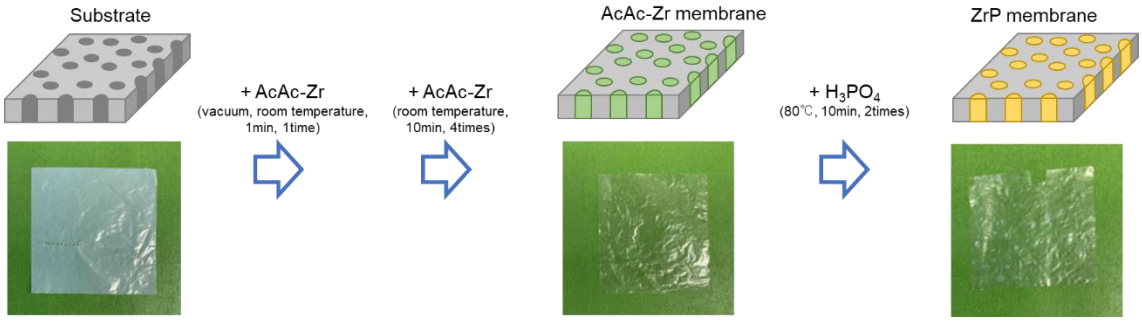

Fig. 1 The step to fabricate a ZrP pore-filling membrane (pore size: 30 nm)

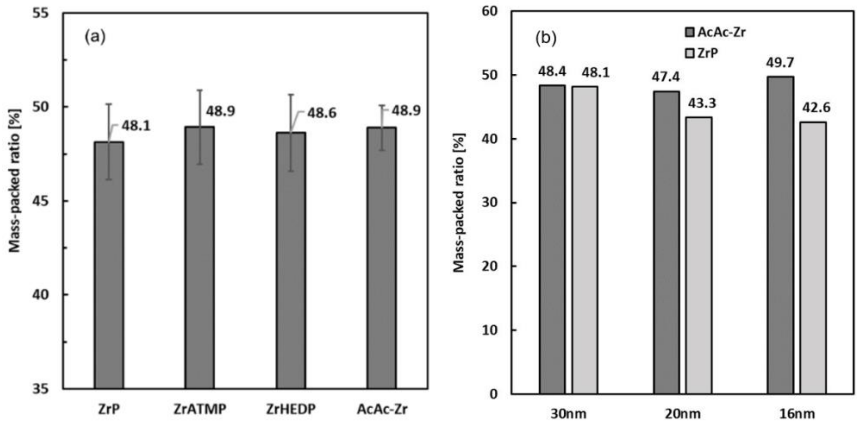

Fig. 2 Pore-filling ratio of (a) the ZrP/ZrATMP/ZrHEDP/AcAc-Zr membrane (pore size: 30 nm), (b) the AcAc-Zr membrane with different pore size

3.1.2 FT-IR analysis

ZrP-based inorganics were confirmed by FT-IR analysis. The FT-IR spectra of the ZrP/ZrHEDP/ZrATMP membrane, the substrate, and the AcAc-Zr membrane are shown in Fig. 3. The spectrum of the AcAc-Zr membrane has a C=C=C resonance peak (1524 cm^{-1}) [47] and amorphous Zr-O bonds (around 650 cm^{-1}) [48]. The spectra of the ZrP/ZrATMP/ZrHEDP membranes have a peak derived from the primary P-O phosphate bond (900~1300cm^{-1}). For the ZrP membrane, the characteristic peak at 1250 cm^{-1} is due to stretching vibration by P-O-H, the absorption peak at 1620 cm^{-1} is due to the asymmetric stretching vibration of O-H in the layered crystal of α-ZrP, and the peak at 596 cm is due to Zr-O bonding [49], [50]. The peaks at 596 cm^{-1} and at 530 cm^{-1} are due to Zr-O bonding and PO_4^-, respectively [44].

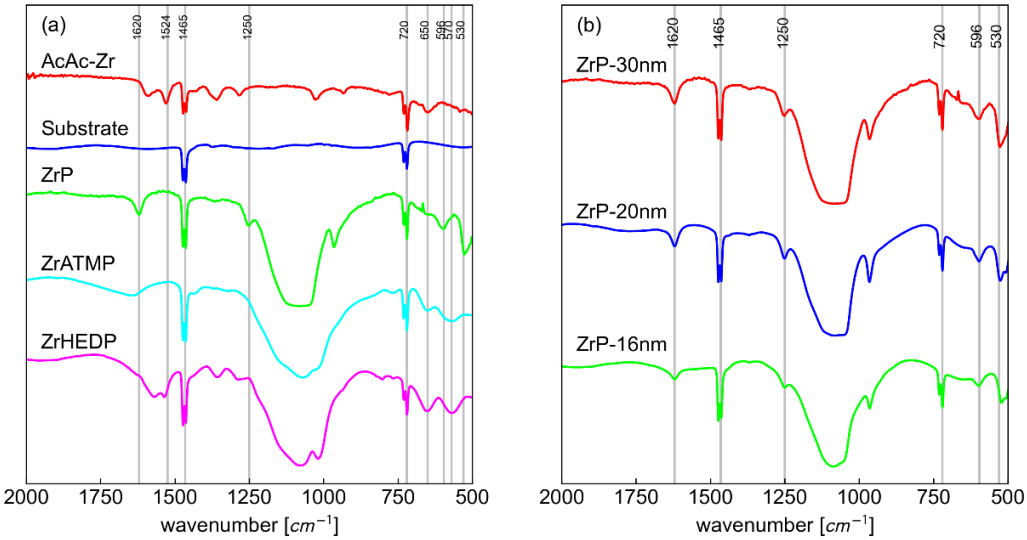

Fig.3 FT-IR spectrum of (a) the AcAc-Zr/ZrP/ZrATMP/ZrHEDP membrane and the substrate (pore size: 30 nm), (b) the ZrP membrane with different pore sizes (30 nm, 20 nm, 16 nm)

3.1.3 ZrP structure of XRD

Fig. 4 shows the XRD patterns of the substrate, the AcAc-Zr powder, and the ZrP/ZrATMP/ZrHEDP membranes. No characteristic peaks exist in the XRD pattern of AcAc-Zr powder, implying that AcAc-Zr has an amorphous state. All membranes have sharp peaks at 2θ = 21.6° and 24.0°, derived from the PE substrate [50], [51]. On the other hand, ZrP membranes have peaks at 2θ = 11.4°, 19.9°, 25.0°, and 34.0°, regardless of the pore size. These peaks correspond to the (002), (110), (112), and (303) lattice planes of α-ZrP crystal [52]. The lattice constant corresponding to 2θ = 11.4° under the condition of first-order diffraction (n = 1) in the Bragg's equation (4) is $d \approx 7.76$ Å. This value is in good agreement with the lattice spacing of α-ZrP crystals ($d = 7.6$ Å) reported previously [53].

$$2d \sin\theta = n\lambda \tag{4}$$

(d: distance between crystal faces [nm], θ: angle between crystal face and X-ray [degree],
λ: wavelength of X-ray [nm], n: natural number)

On the other hand, for the ZrATMP and ZrHEDP membranes, no characteristic peaks are found other than peaks of PE and AcAc-Zr. It means that ZrATMP and ZrHEDP exist in an amorphous state in the membranes.

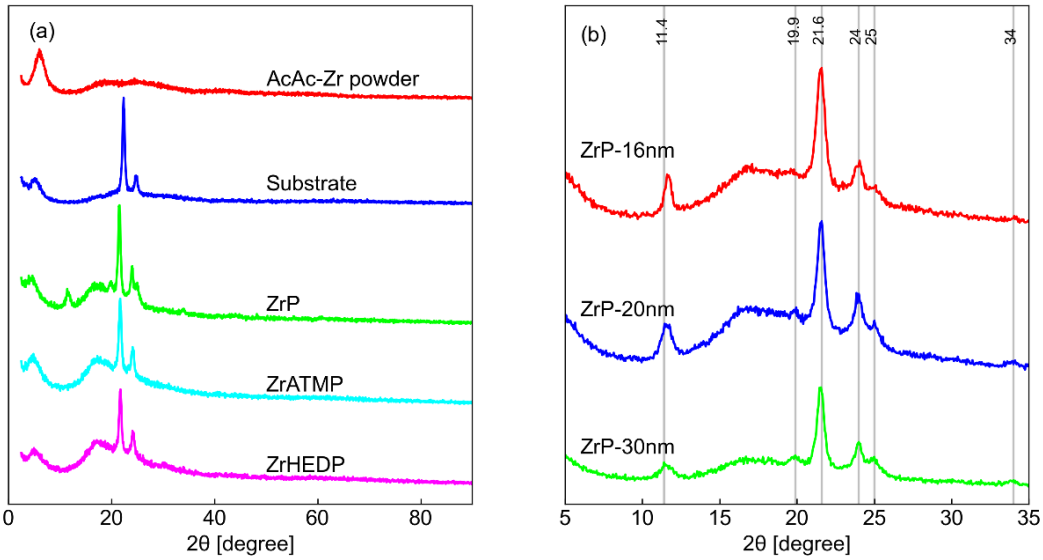

Fig.4 XRD of (a) the AcAc-Zr powder, the substrate, and the membrane with ZrP-derivatives (pore size: 30 nm), (b) the ZrP membrane with different pore sizes (30 nm, 20 nm, 16 nm)

3.1.4 SEM/TEM/EDS

Fig. 5 shows SEM/TEM/EDS images of the ZrP membrane and the substrate with an average pore size of 30 nm. Fig. 5(a) presents the texture of pores on the substrate before pore-filling, while Fig. 5(b) indicates a smooth surface after pore-filling of ZrP. Fig. 5(c) shows the cross-section of the ZrP membrane where 30 nm-pores are filled with layered crystals, identified as ZrP by EDS results in Fig. 5(d): the white region is the substrate, and the black region is ZrP. The layered crystals are connected to each other, and percolation of ZrP is formed. Table 1 gives EDS results of the cross-section of the ZrP membrane, indicating that about 40 wt.% of the membrane is composed of O, P, and Zr atoms in the range of the image. In addition, the molar ratio of P and Zr is almost the same.

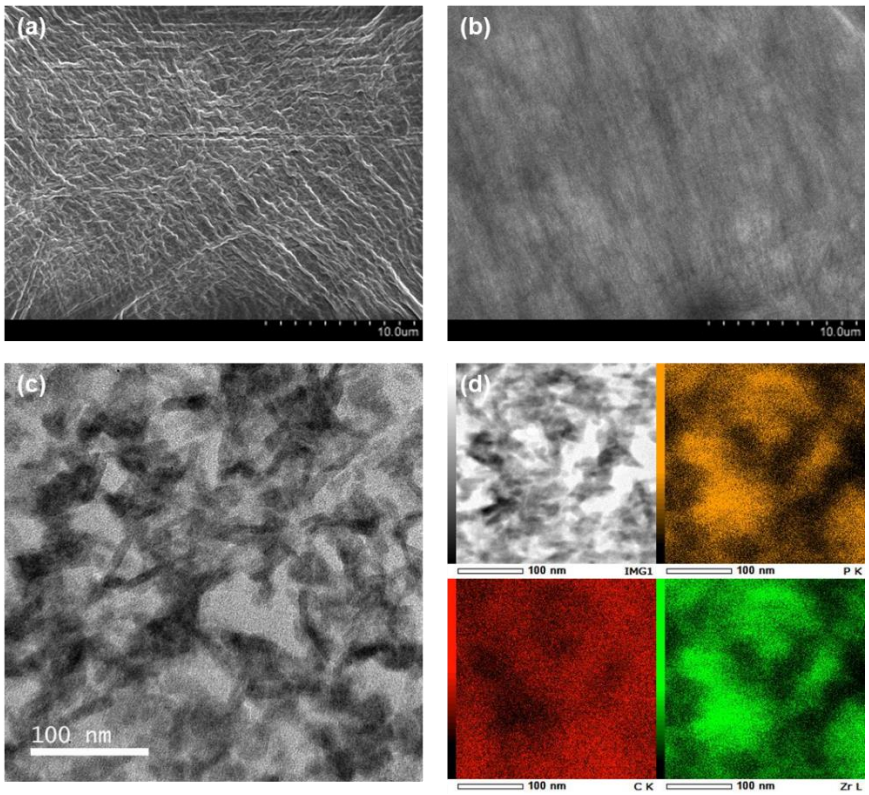

Fig.5 SEM/TEM/TEM-EDS of the ZrP membrane and SEM of the pristine substrate (pore size: 30nm): (a) SEM of the substrate before pore-filling, (b) SEM of the ZrP membrane, (c) TEM of the ZrP membrane, (d) EDS of the ZrP membrane

Table 1 EDS composition analysis of the cross-section of ZrP membrane

Elements	Mass (wt.%)	σ (wt.%)	Atomic ratio (%)
C	59.05	0.04	77.88
O	15.45	0.03	15.30
P	7.09	0.02	3.62
Zr	18.41	0.07	3.20

3.2 Membrane conductivity

The following Fig.5 shows the proton conductivity of the membranes with a pore size of 30 nm. The conductivities of ZrP, ZrATMP, and ZrHEDP are 3.4±0.6 mS cm^{-1}, 0.8±0.2 mS cm^{-1}, 6.3±1.3 mS cm^{-1} , respectively.

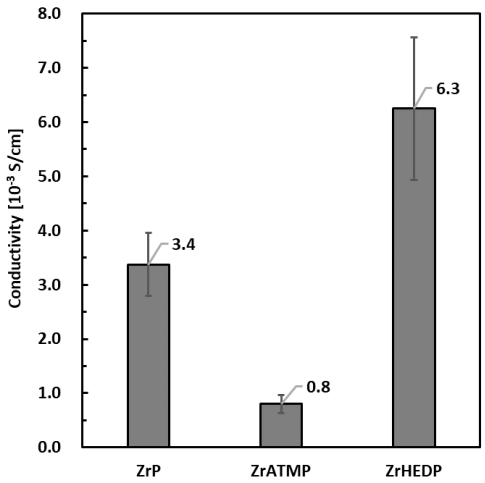

Fig.6 Proton conductivity result of the ZrP/ZrATMP/ZrHEDP membrane (pore size: 30 nm) at 80°C and 95%RH

4. Discussion

4.1 Origin of high pore-filling ratio in substrates with different pore

Fig. 2 revealed that AcAc-Zr was filled in the porous substrates with a large amount, about 48 wt.%, when the pore size of the substrate is 30 nm or less. The size of AcAc-Zr is small, about 2~5 nm [17], and thus it is reasonable that Acac-Zr occupies the pores. In contrast, the substrates with a pore size of 50 nm, 70 nm, and 100 nm could not be filled and their transparency did not change after pore-fillling. It is an intriguing phenomenon because the smaller pore should be more difficult to be filled than larger pores, although the results are opposite. The plausible explanation is the hydrophobic interaction between AcAc groups and PE substrate. The surface area of the 30 nm substrate is larger than that of the 50 nm substrate when their porosity is the same, resulting in more hydrophobic interaction based on the Acac-chelating. Therefore, the surface modification for the interaction seems essential to fill singly inorganic into a substrate at high contents.

On the other hand, after the conversion to ZrP, the 30 nm substrate showed the highest pore-filling ratio, while the ratio of ZrP decreased in the substrates with smaller pore diameters. It might be because the reaction condition is suitable for conversion to ZrP in the 30 nm substrate. Since PE is hydrophobic, the hydrophobic surface area could increase as the pore size of the substrate decreases, which is expected to increase the hydrophobicity of the substrate surface. This effect could make it difficult for hydrophilic compounds such as phosphoric acid, a reactant of ZrP, to penetrate the substrate. As a result, the chemical reaction between AcAc-Zr and phosphoric acid did not occur sufficiently. It suggests that it could be possible to successfully convert 20 nm/16 nm AcAc-Zr membranes to the ZrP membranes retaining the high pore-filling ratio by increasing nonpolar solvent in phosphoric acid solution.

There are two main advantages of high inorganic content membranes with smaller pore sizes. The first advantage is that when the pore size is small, the hydrophobicity is increased due to the original property of PE. As a result, hydrophilic solution permeation could be reduced. The second advantage is that the pore size is smaller, the surface area of the PE is larger, and the surface area of the ZrP filled in the PE is larger accordingly. Thus, the counter-ion on the ZrP surface, which efficiently conduct protons, can be increased. Previous studies proved that in ZrP crystals, the counter-ions on the surface are 10^4 times more likely to transport current than the ions inside [54]. Therefore, if the substrate with a larger surface area, namely, with smaller pore sizes, can be filled with a higher concentration of ZrP, a higher conductivity could be achieved.

4.2 Various inorganics in the membrane

Fig. 2 revealed that the prepared membrane contains inorganics with a high pore-filling ratio, about 48 wt.%. Furthermore, the TEM image shows that the hydrophobic phase (PE) and the hydrophilic phase (ZrP) are well separated from each other and that the ZrP crystals are connected to form the continuous proton transfer pathways. On the other hand, most of the inorganic-organic composite membranes studied so far have a mass ratio of about 10-15 wt.% [24], [55], [56]. In addition, few inorganic-organic composite membranes synthesized have well-connected proton pathways [11], [22], [33], [44], [45], [56], [57]. Therefore, the ZrP membrane fabricated in this study is of great importance. There is also a remarkable discovery: three types of inorganic particles, ZrP/ZrATMP/ZrHEDP, can be packed into the substrates at a high concentration of about 48 wt.% with the same technique. It is expected that various ZrP-based inorganic particles can be packed into the substrate by converting Acac-Zr. As we mentioned in the introduction, those inorganic particles have a variety of possible applications. Even if the application is not for PEM, the phase-separated structure is beneficial because the structure does not leave isolated inorganics and maximizes its properties. The presented method can easily be applied to fill a large amount of multiple inorganic particles with continuous structure.

4.3 Proton conductivity of the ZrP/ZrATMP/ZrHEDP membrane

Fig. 6 showed that the proton conductivity of the ZrP membrane is 3.4 mS cm^{-1} at 80°C and 95%RH. The conductivity of the ZrP crystal itself is known to be about 0.3 mS cm^{-1} at 90°C and 90%RH from a previous study, and it is also known that the conductivity of various ZrP-PTFE films is about 0.1~10 mS cm^{-1} [17], [45], [60]. In addition, considering that the porosity of the substrate used in this study is 55% (pore size: 30 nm), the conductivity of the ZrP membrane is sufficiently high. It may be due to the effect of the counter-ions on the surface of ZrP crystals, as described in 4.1. Furthermore, the thickness of the membrane synthesized in this study is 7~10 μm, which is beneficial because the resistance of the membranes in PEMFC is reduced by making PEMs thinner [61]. The thickness of the Nafion® film is about 50-150 μm, and that of most of the PEMs reported so far is about 50 μm thick [45], [60]. It is because if a film becomes thinner, its strength cannot be sufficiently maintained, and at the same time, fuel permeation is likely to occur. On the other hand, the membrane synthesized in this study is durable because of the strong PE backbone and the high ZrP content in relatively small pores (less than 30 nm), which should reduce fuel permeation.

4.4 Remained issues

Table 1 implies that the conversion efficiency of AcAc-Zr to ZrP is not high enough. Theoretically, if ideal $Zr(HPO_4)_2 \cdot H_2O$, α-ZrP, exists in the film, the ratio of the number of atoms should be Zr : P : O = 1 : 2 : 9. However, as shown in Table 1, the composition analysis of the ZrP film prepared in this study shows that the ratio is Zr : O : P = 1.0 : 1.1 : 4.8, which indicates that only about 50% of AcAc-Zr reacts in the area observed by the EDS results. If the unreacted AcAc-Zr can be reduced, the conductivity of the ZrP film should be further increased, which is a future task.

5. Conclusion

In this study, we fabricated a pore-filling membrane with a high concentration of ZrP derivatives (> 48 wt.%) with percolated structures by a simple method: filling AcAc-Zr into the substrate and converting AcAc-Zr to ZrP in situ. The high pore-filling ratio of ZrP in the membrane demonstrated high proton conductivity (3.4±0.6 mS cm^{-1}). Furthermore, it was confirmed that ZrATMP/ZrHEDP films could be prepared by the same method. It indicates a possibility that membranes containing various ZrP-based inorganic particles can be readily obtained by modifying the reactant in the conversion. There are many possible applications of membranes containing ZrP derivatives, not only as proton conductors for PEMFC but also as catalysts, harmful ion removal, antibacterial materials, and support materials for SSAs. Therefore, the method developed in this study can be a platform for functional membranes based on diverse ZrP derivatives with high contents and percolated structure.

Author statement

[†]T. T. and T. O. contributed equally to this work.

Declaration of competing interest

The authors declare that they have no known competing financial interests or personal relationships that could have appeared to influence the work reported in this paper.

Acknowledgments

The authors acknowledge helpful assistance with TEM-EDS analysis from Dr. Yasunori Hayashi.

Appendix

The following figure is part of the Cole-Cole plot obtained from the AC impedance measurement.

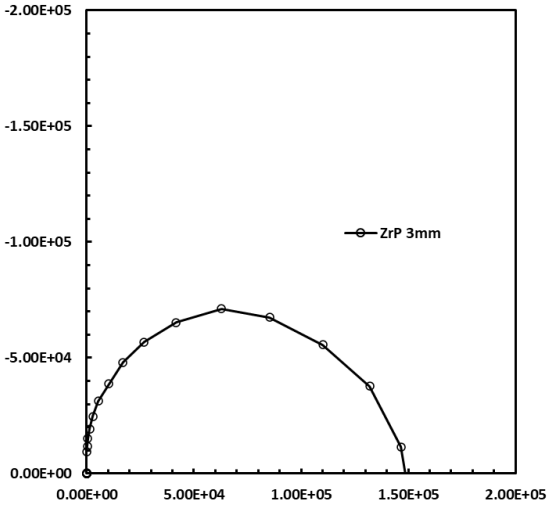

References

[1] R. Kumar, M. Ahmed, G. Bhadrachari, S. Al- Muqahwi, and J. P. Thomas, "Thin-film nanocomposite membrane comprised of a novel phosphonic acid derivative of titanium dioxide for efficient boron removal," *Journal of Environmental Chemical Engineering*, vol. 9, no. 4, Aug. 2021, doi: 10.1016/j.jece.2021.105722.

[2] X. Cheng *et al.*, "Ultrahigh-flux and self-cleaning composite membrane based on BiOCl-PPy modified MXene nanosheets for contaminants removal from wastewater," *Journal of Membrane Science*, vol. 644, Feb. 2022, doi: 10.1016/j.memsci.2021.120188.

[3] H. Zhang, X. Quan, S. Chen, H. Zhao, and Y. Zhao, "Fabrication of photocatalytic membrane and evaluation its efficiency in removal of organic pollutants from water," *Separation and Purification Technology*, vol. 50, no. 2, pp. 147–155, Jun. 2006, doi: 10.1016/j.seppur.2005.11.018.

[4] H. W. Abu El Hawa, S. N. Paglieri, C. C. Morris, A. Harale, and J. Douglas Way, "Application of a Pd-Ru composite membrane to hydrogen production in a high temperature membrane reactor," *Separation and Purification Technology*, vol. 147, pp. 388–397, Jun. 2015, doi: 10.1016/j.seppur.2015.02.005.

[5] E. Kikuchi, "Membrane reactor application to hydrogen production," 2000.

[6] Y. S. Jo *et al.*, "A viable membrane reactor option for sustainable hydrogen production from ammonia," *Journal of Power Sources*, vol. 400, pp. 518–526, Oct. 2018, doi: 10.1016/j.jpowsour.2018.08.010.

[7] S. Zhang *et al.*, "A porous, mechanically strong and thermally stable zeolitic imidazolate framework-8@bacterial cellulose/aramid nanofibers composite separator for advanced lithium-ion batteries," *Journal of Membrane Science*, vol. 652, p. 120461, Jun. 2022, doi: 10.1016/j.memsci.2022.120461.

[8] R. Kim *et al.*, "Ultrathin Nafion-filled porous membrane for zinc/bromine redox flow batteries," *Scientific Reports*, vol. 7, no. 1, Dec. 2017, doi: 10.1038/s41598-017-10850-9.

[9] J. J. Sumner, S. E. Creager, J. J. Ma, and D. D. Desmarteau, "Proton Conductivity in Nafion® 117 and in a Novel BisE (perfl uoroalkyl)sulf onyl]im ide lonomer Membrane," 1998.

[10] Y. Kim, K. Ketpang, S. Jaritphun, J. S. Park, and S. Shanmugam, "A polyoxometalate coupled graphene oxide-Nafion composite membrane for fuel cells operating at low relative humidity," *Journal of Materials Chemistry A*, vol. 3, no. 15, pp. 8148–8155, Apr. 2015, doi: 10.1039/c5ta00182j.

[11] K. Oh, O. Kwon, B. Son, D. H. Lee, and S. Shanmugam, "Nafion-sulfonated silica composite membrane for proton

exchange membrane fuel cells under operating low humidity condition," *Journal of Membrane Science*, vol. 583, pp. 103–109, Aug. 2019, doi: 10.1016/j.memsci.2019.04.031.

[12] Z. Li *et al.*, "Enhanced proton conductivity of nafion hybrid membrane under different humidities by incorporating metal-organic frameworks with high phytic acid loading," *ACS Applied Materials and Interfaces*, vol. 6, no. 12, pp. 9799–9807, Jun. 2014, doi: 10.1021/am502236v.

[13] F. Bauer and M. Willert-Porada, "Characterisation of zirconium and titanium phosphates and direct methanol fuel cell (DMFC) performance of functionally graded Nafion(R) composite membranes prepared out of them," *Journal of Power Sources*, vol. 145, no. 2, pp. 101–107, Aug. 2005, doi: 10.1016/j.jpowsour.2005.01.063.

[14] B. P. Tripathi and V. K. Shahi, "Organic-inorganic nanocomposite polymer electrolyte membranes for fuel cell applications," *Progress in Polymer Science (Oxford)*, vol. 36, no. 7. Elsevier Ltd, pp. 945–979, 2011. doi: 10.1016/j.progpolymsci.2010.12.005.

[15] A. Clearfield, "Role of Ion Exchange in Solid-State Chemistry," 1988. [Online]. Available: https://pubs.acs.org/sharingguidelines

[16] K. B. Mangat, E. L. Whelton, S. F. Hache, J. I. Malone, C. H. Lindley, and G. Alberti, "Tetravalent Metal Salts 163 several U.N.B. undergraduate students whose work in various unpublished areas of the topic has gone unacknowledged previously. These are Syntheses, Crystalline Structure, and Ion-Exchange Properties of Insoluble Acid Salts of Tetravalent Metals and Their Salt Forms," 1978. [Online]. Available: https://pubs.acs.org/sharingguidelines

[17] J. M. Lee, Y. Kikuchi, H. Ohashi, T. Tamaki, and T. Yamaguchi, "Novel mild conversion routes of surface-modified nano zirconium oxide precursor to layered proton conductors," *Journal of Materials Chemistry*, vol. 20, no. 30, pp. 6239–6244, Aug. 2010, doi: 10.1039/c0jm00130a.

[18] U. Costantino, R. Vivani, V. Zima, and E. Cernoskova, "Thermoanalytical Study, Phase Transitions, and Dimensional Changes of-Zr(HPO 4) 2 · H 2 O Large Crystals," 1997.

[19] M. Aparicio, J. Mosa, and A. Durán, "Hybrid organic-inorganic nanostructured membranes for high temperature proton exchange membranes fuel cells (PEMFC)," in *Journal of Sol-Gel Science and Technology*, Dec. 2006, vol. 40, no. 2–3, pp. 309–315. doi: 10.1007/s10971-006-8370-2.

[20] R. Vendamme, S. Y. Onoue, A. Nakao, and T. Kunitake, "Robust free-standing nanomembranes of organic/inorganic interpenetrating networks," *Nature Materials*, vol. 5, no. 6, pp. 494–501, Jun. 2006, doi: 10.1038/nmat1655.

[21] Y. M. Kim, S. H. Choi, H. C. Lee, M. Z. Hong, K. Kim, and H. I. Lee, "Organic-inorganic composite membranes as addition of SiO2 for high temperature-operation in polymer electrolyte membrane fuel cells (PEMFCs)," *Electrochimica Acta*, vol. 49, no. 26, pp. 4787–4796, Oct. 2004, doi: 10.1016/j.electacta.2004.05.034.

[22] Ju-Myeung Lee, Hidenori Ohashi, Taichi Ito, and Takeo Yamaguchi, "Morphological Investigations of Surface Modified Zirconia Precursor by Perfluorosulfonated Ionomer Using Nano Capping Technique," *JOURNAL OF CHEMICAL ENGINEERING OF JAPAN*, vol. 42, no. 12, pp. 918–929, 2009.

[23] G. M. Anilkumar, S. Nakazawa, T. Okubo, and T. Yamaguchi, "Proton conducting phosphated zirconia-sulfonated polyether sulfone nanohybrid electrolyte for low humidity, wide-temperature PEMFC operation," *Electrochemistry Communications*, vol. 8, no. 1, pp. 133–136, Jan. 2006, doi: 10.1016/j.elecom.2005.10.025.

[24] Y. Özdemir, N. Üregen, and Y. Devrim, "Polybenzimidazole based nanocomposite membranes with enhanced proton conductivity for high temperature PEM fuel cells," *International Journal of Hydrogen Energy*, vol. 42, no. 4, pp. 2648–2657, Jan. 2017, doi: 10.1016/j.ijhydene.2016.04.132.

[25] M. Pica, "Zirconium phosphate catalysts in the XXI century: State of the art from 2010 to date," *Catalysts*, vol. 7, no. 6. MDPI, Jun. 19, 2017. doi: 10.3390/catal7060190.

[26] W. Y. Hsu and T. D. Gierke, "ION TRANSPORT AND CLUSTERING IN NAFION* PERFLUORINATED MEMBRANES**," 1983.

[27] T. Ogawa, K. Kamiguchi, T. Tamaki, H. Imai, and T. Yamaguchi, "Differentiating Grotthuss proton conduction mechanisms by nuclear magnetic resonance spectroscopic analysis of frozen samples," *Analytical Chemistry*, vol. 86, no. 19, pp. 9362–9366, Oct. 2014, doi: 10.1021/ac5021485.

[28] T. Ogawa *et al.*, "The proton conduction mechanism in a material consisting of packed acids," *Chemical Science*, vol. 5, no. 12, pp. 4878–4887, Dec. 2014, doi: 10.1039/c4sc00952e.

[29] M. Tuckerman, K. Laasonen, M. Sprik, and M. Parrinello, "Ab initio molecular dynamics simulation of the solvation and transport of hydronium and hydroxyl ions in water," *The Journal of Chemical Physics*, vol. 103, no. 1, pp. 150–161, 1995, doi: 10.1063/1.469654.

[30] M. Tuckerman, K. Laasonen, M. Sprik, and M. Parrinello1, "Ab Initio Molecular Dynamics Simulation of the Solvation and Transport of H30+ and OH Ions in Water," 1995. [Online]. Available: https://pubs.acs.org/sharingguidelines

[31] T. Ogawa, H. Ohashi, G. M. Anilkumar, T. Tamaki, and T. Yamaguchi, "Suitable acid groups and density in electrolytes to facilitate proton conduction," *Physical Chemistry Chemical Physics*, vol. 23, no. 41, pp. 23778–23786, Nov. 2021, doi: 10.1039/d1cp00718a.

[32] T. Ogawa, "Ammonia as a carrier of renewable energy: Recent progress of ammonia synthesis by homogeneous catalysts, heterogeneous catalysts, and electrochemical method," in *Emerging Trends to Approaching Zero Waste*, Elsevier, 2022, pp. 265–291. doi: 10.1016/b978-0-323-85403-0.00010-4.

[33] Q. Tai, Y. Kan, L. Chen, W. Xing, Y. Hu, and L. Song, "Morphologies and thermal properties of flame-retardant polystyrene/α-zirconium phosphate nanocomposites," *Reactive and Functional Polymers*, vol. 70, no. 6, pp. 340–345, Jun. 2010, doi: 10.1016/j.reactfunctpolym.2010.02.008.

[34] T. Yamaguchi, S.-I. Nakao, and S. Kimura, "Plasma-Graft Filling Polymerization: Preparation of a New Type of Pervaporation Membrane for Organic Liquid Mixtures," 1991. [Online]. Available: https://pubs.acs.org/sharingguidelines

[35] H. Xiao and S. Liu, "Zirconium phosphate (ZrP)-based functional materials: Synthesis, properties and applications," *Materials and Design*, vol. 155, pp. 19–35, Oct. 2018, doi: 10.1016/j.matdes.2018.05.041.

[36] R. K. Nagarale, W. Shin, and P. K. Singh, "Progress in ionic organic-inorganic composite membranes for fuel cell applications," *Polymer Chemistry*, vol. 1, no. 4. pp. 388–408, Jun. 2010. doi: 10.1039/b9py00235a.

[37] M. Pica, "Zirconium phosphate catalysts in the XXI century: State of the art from 2010 to date," *Catalysts*, vol. 7, no. 6. MDPI, Jun. 19, 2017. doi: 10.3390/catal7060190.

[38] F. Ferlin, M. Cappelletti, R. Vivani, M. Pica, O. Piermatti, and L. Vaccaro, "Au@zirconium-phosphonate nanoparticles as an effective catalytic system for the chemoselective and switchable reduction of nitroarenes," *Green Chemistry*, vol. 21, no. 3, pp. 614–626, 2019, doi: 10.1039/c8gc03513j.

[39] E. Abdulkarem *et al.*, "Polyvinylidene fluoride (PVDF)-α-zirconium phosphate (α-ZrP) nanoparticles based mixed matrix membranes for removal of heavy metal ions," *Chemosphere*, vol. 267, Mar. 2021, doi: 10.1016/j.chemosphere.2020.128896.

[40] B. C. Pan *et al.*, "Highly effective removal of heavy metals by polymer-based zirconium phosphate: A case study of lead ion," *Journal of Colloid and Interface Science*, vol. 310, no. 1, pp. 99–105, Jun. 2007, doi: 10.1016/j.jcis.2007.01.064.

[41] M. Nocchetti *et al.*, "Synthesis, Crystal Structure, and Antibacterial Properties of Silver-Functionalized Low-Dimensional Layered Zirconium Phosphonates," *Inorganic Chemistry*, vol. 61, no. 4, pp. 2251–2264, Jan. 2022, doi: 10.1021/acs.inorgchem.1c03565.

[42] M. Taddei, P. Sassi, F. Costantino, and R. Vivani, "Amino-Functionalized Layered Crystalline Zirconium

Phosphonates: Synthesis, Crystal Structure, and Spectroscopic Characterization," *Inorganic Chemistry*, vol. 55, no. 12, pp. 6278–6285, Jun. 2016, doi: 10.1021/acs.inorgchem.6b00943.

[43] G. Alberti and M. Casciola, "Composite membranes for medium-temperature PEM fuel cells," *Annual Review of Materials Research*, vol. 33, pp. 129–154, 2003, doi: 10.1146/annurev.matsci.33.022702.154702.

[44] J. Pandey, M. M. Seepana, and A. Shukla, "Zirconium phosphate based proton conducting membrane for DMFC application," *International Journal of Hydrogen Energy*, vol. 40, no. 30, pp. 9410–9421, Aug. 2015, doi: 10.1016/j.ijhydene.2015.05.117.

[45] A. Al-Othman, A. Y. Tremblay, W. Pell, Y. Liu, B. A. Peppley, and M. Ternan, "The effect of glycerol on the conductivity of Nafion-free ZrP/PTFE composite membrane electrolytes for direct hydrocarbon fuel cells," *Journal of Power Sources*, vol. 199, pp. 14–21, Feb. 2012, doi: 10.1016/j.jpowsour.2011.09.104.

[46] H. Han, U. Bach, Y. B. Cheng, and R. A. Caruso, "Increased nanopore filling: Effect on monolithic all-solid-state dye-sensitized solar cells," *Applied Physics Letters*, vol. 90, no. 21, 2007, doi: 10.1063/1.2743381.

[47] W.-K. Kuo and Y.-C. Ling, "Effects of mono-substituting chelating agents on BaTi03 prepared by the sol-gel process," 1994.

[48] J. M. Lin, M. chi Hsu, and K. Z. Fung, "Deposition of ZrO2 film by liquid phase deposition," *Journal of Power Sources*, vol. 159, no. 1 SPEC. ISS., pp. 49–54, Sep. 2006, doi: 10.1016/j.jpowsour.2006.04.116.

[49] R. Gloukhovski, V. Freger, and Y. Tsur, "Understanding methods of preparation and characterization of pore-filling polymer composites for proton exchange membranes: A beginner's guide," *Reviews in Chemical Engineering*, vol. 34, no. 4, pp. 455–479, Jul. 2018, doi: 10.1515/revce-2016-0065.

[50] L. Zhou, X. Wang, Y. Zhang, P. Zhang, and Z. Li, "An experimental study of the crystallinity of different density polyethylenes on the breakdown characteristics and the conductance mechanism transformation under high electric field," *Materials*, vol. 12, no. 7, 2019, doi: 10.3390/ma12172657.

[51] K. T. Li and L. H. Wu, "Constrained geometry organotitanium catalysts supported on nanosized silica for ethylene (co)polymerization," *Molecules*, vol. 22, no. 5, May 2017, doi: 10.3390/molecules22050751.

[52] J. M. Lee, Y. Kikuchi, H. Ohashi, T. Tamaki, and T. Yamaguchi, "Novel mild conversion routes of surface-modified nano zirconium oxide precursor to layered proton conductors," *Journal of Materials Chemistry*, vol. 20, no. 30, pp. 6239–6244, Aug. 2010, doi: 10.1039/c0jm00130a.

[53] H. J. Sue, K. T. Gam, N. Bestaoui, N. Spurr, and A. Clearfield, "Epoxy Nanocomposites Based on the Synthetic α-Zirconium Phosphate Layer Structure," *Chemistry of Materials*, vol. 16, no. 2, pp. 242–249, Jan. 2004, doi: 10.1021/cm030441s.

[54] G. Alberti, M. Casciola, U. Costantino, G. Levi, and G. Ricciardi, "ON THE MECHANISM OF DIFFUSION AND IONIC TRANSPORT IN CRYSTALLINE INSOLUBLE ACID SALTS OF TETRAVALENT METALS-It ELECTRICAL CONDUCTANCE OF ZIRCONIUM BIS (MONOHYDROGEN ORTHO-PHOSPHATE) MONOHYDRATE WITH A LAYERED STRUCTURE," Pergamon Press, 1978.

[55] R. He, Q. Li, G. Xiao, and N. J. Bjerrum, "Proton conductivity of phosphoric acid doped polybenzimidazole and its composites with inorganic proton conductors," *Journal of Membrane Science*, vol. 226, no. 1–2, pp. 169–184, Dec. 2003, doi: 10.1016/j.memsci.2003.09.002.

[56] S. P. Nunes, B. Ruffmann, E. Rikowski, S. Vetter, and K. Richau, "Inorganic modification of proton conductive polymer membranes for direct methanol fuel cells," 2002.

[57] T. Ogawa, T. Tamaki, and T. Yamaguchi, "Proton conductivity of organic-inorganic electrolyte for polymer electrolyte fuel cell," *Chemistry Letters*, vol. 46, no. 2, pp. 204–206, 2017, doi: 10.1246/cl.160935.

[58] T. Ogawa, T. Tamaki, and T. Yamaguchi, “Proton conductivity of organic-inorganic electrolyte for polymer electrolyte fuel cell,” *Chemistry Letters*, vol. 46, no. 2, pp. 204–206, 2017, doi: 10.1246/cl.160935.

[59] T. Nakajima, T. Tamaki, H. Ohashi, and T. Yamaguchi, “ Introduction of Size-Controlled Nafion/ZrO 2 Nanocomposite Electrolyte into Primary Pores for High Pt Utilization in PEFCs ,” *Journal of The Electrochemical Society*, vol. 160, no. 2, pp. F129–F134, 2013, doi: 10.1149/2.065302jes.

[60] Y.-I. Park, J.-D. Kim, and M. Nagai, “High proton conductivity in ZrP-PTFE composites.”

[61] Y. Oshiba, J. Tomatsu, and T. Yamaguchi, “Thin pore-filling membrane with highly packed-acid structure for high temperature and low humidity operating polymer electrolyte fuel cells,” *Journal of Power Sources*, vol. 394, pp. 67–73, Aug. 2018, doi: 10.1016/j.jpowsour.2018.05.013.